PHYSICAL REVIEW B VOLUME 42, NUMBER 14 15 NOVEMBER 1990-I

Electric-field effects on exciton lifetimes in symmetric coupled $GaAs/Al_{0.3}Ga_{0.7}As$ double quantum wells

A. Alexandrou, J. A. Kash, E. E. Mendez, M. Zachau, and J. M. Hong
IBM Research Division, Thomas J. Watson Research Center, P.O. Box 218, Yorktown Heights, New York 10598

T. Fukuzawa and Y. Hase
IBM Research Division, Tokyo Research Laboratory, Sanban-cho, Tokyo 102, Japan

(Received 16 July 1990)

We have studied the effects of coupling on the lifetime of spatially indirect excitons in (50-Å GaAs)/$Al_{0.3}Ga_{0.7}As$ symmetric double quantum wells. The coupling was controlled by varying the barrier thickness between 25 and 60 Å and by application of an electric field. Lifetime enhancements of up to 3 orders of magnitude relative to the lifetimes of spatially direct excitons were observed. At a given electric field the lifetime enhancement was larger the wider the barrier, due to the smaller electron-hole wave-function overlap, in good agreement with theory. We have also observed nonresonant hole tunneling and estimated the tunneling time, which was of the order of 300 ps in a 40-Å-barrier sample.

Application of an electric field perpendicular to the layers of a quantum-well structure drastically changes the exciton recombination lifetime. Large increases of the recombination lifetime have been observed in single quantum wells[1] due to the field-induced polarization of electron-hole pairs and the subsequent reduction in the electron-hole wave-function overlap. In coupled double quantum wells (DQW) the electric field leads to the formation of spatially indirect excitons with electrons localized in one well and holes localized in the other[2,3] (see Fig. 1). Recombination lifetimes associated with these indirect excitons have been reported to be much longer than those of spatially direct excitons, in symmetric[4] as well as in asymmetric DQW.[5,6]

It has been theoretically predicted that these long-lived spatially indirect excitons can undergo Bose condensation.[7] The long lifetimes should allow thermalization and condensation to occur before the electron-hole recombination. Furthermore, the separation of electrons and holes in two different wells should prevent the formation of exciton molecules or drops. In addition, experimental indications of an electric-field-induced phase transition, manifested by an abrupt reduction of the photoluminescence linewidth in a DQW structure with 50-Å GaAs wells separated by a 40-Å $Al_{0.3}Ga_{0.7}As$ barrier, have recently been reported.[8]

Thus, the detailed knowledge of the exciton lifetimes in coupled DQW systems under electric fields becomes crucial for the determination of the relevance of the field-induced lifetime enhancement in this phase transition. In this work, we present time-resolved luminescence measurements in $GaAs/Al_{0.3}Ga_{0.7}As$ symmetric coupled DQW under electric field and compare the results for different barrier thicknesses with theoretical calculations based on the spatial electron-hole wave-function overlap.

We have also observed heavy-hole nonresonant tunneling between the two wells. Hole tunneling in heterostructures is a field of growing interest,[9–14] especially after recent theoretical work[15–18] predicting much faster hole tunneling times than generally accepted,[19] due to the mixing between the heavy- and light-hole bands. The tunneling time deduced here is of the order of 300 ps for a symmetric DQW structure with a 40-Å barrier under an electric field of 16 kV/cm, an estimation that agrees with calculations in the same kind of structure.[18]

The three samples used in this study were grown by

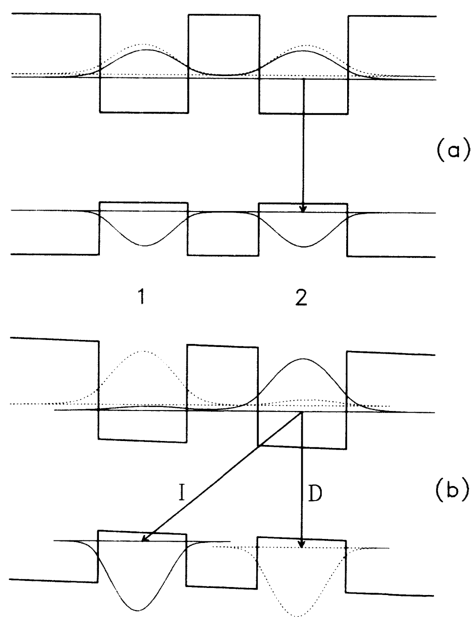

FIG. 1. Potential profile and electron and heavy-hole squared wave functions for a double quantum-well structure with 50-Å GaAs wells and a 40-Å $Al_{0.3}Ga_{0.7}As$ barrier (50 Å–40 Å–50 Å) (a) under flat-band conditions and (b) for an electric field of 15 kV/cm. The wave functions were calculated by numerically solving Schrödinger's equation. The arrows show the transitions observed in photoluminescence. Solid (dashed) lines denote the symmetric (antisymmetric) states. Under flat-band conditions the antisymmetric heavy-hole state cannot be distinguished from the symmetric one. D (I) denotes the spatially direct (indirect) transition.

molecular-beam epitaxy and contained ten sets of symmetric DQW. The wells consisted of 50 Å GaAs while the $Al_{0.3}Ga_{0.7}As$ barrier thickness was 25, 40, and 60 Å, respectively, in each of the three samples. The individual DQW units were separated by 200 Å $Al_{0.3}Ga_{0.7}As$ and the whole was clad by 1000-Å $Al_{0.3}Ga_{0.7}As$ layers on both sides. This structure formed the intrinsic layer of a p^+-i-n^+ diode grown on a n^+-type GaAs substrate, thus enabling application of an electric field.

The samples were placed in a immersion-liquid-He cryostat and excited with 5-ps pulses at an 75.6-MHz repetition rate from a Styryl-8 dye laser synchronously pumped by the second harmonic of a mode-locked neodymium-doped yttrium aluminum garnet (Nd^+:YAG) laser. All measurements were performed at a temperature of 1.8 K. The excitation energy and the averaged power density were 1.675 eV and 0.1 W/cm^2, respectively. The photoluminescence was dispersed with a triple spectrometer with a 0.5-m dispersion stage and detected with a cooled imaging photomultiplier tube. The time decay was measured by time-resolved photon-counting using a time-to-amplitude converter. The photon timing signal was taken at the Z-microchannel plate output.[20] The $1/e$ time of the system response curve was 150 ps.

Under flat-band conditions the electron and hole wave functions in a pair of quantum wells separated by a thin enough barrier are extended over both wells. In photoluminescence one transition is observed, corresponding to recombination of electrons and heavy holes in the symmetric state [as marked by the arrow in Fig. 1(a)]. Under moderate electric fields the heavy-hole wave functions are completely localized in one of the two wells, whereas the electron wave functions still partially extend into the neighboring well. Two transitions are observed in photoluminescence, as shown in Fig. 1(b), a spatially indirect one (since the electron wave function is mostly localized in well 2 while the hole wave function is localized in well 1) and a spatially direct one. The direct transition becomes possible because the electric field distorts the wave-function symmetries. At moderate electric fields the indirect transition shifts to lower energies linearly with the electric field $\mathcal{E}$ (the energy shift, ΔE, is equal to $e\mathcal{E}d$, where d is the distance between the centers of the quantum wells and e is the charge of the electron) while the direct one initially moves to slightly higher energies and then remains unchanged.[2]

Figure 2 depicts the time-integrated photoluminescence associated with the two transitions shown in Fig. 1(b) for the three samples studied in this work, each at an electric field of approximately 14 kV/cm. The arrows indicate the peak positions of the luminescence lines under flat-band conditions. The energy of the peak position is expected to be lower as the barrier width decreases, due to the increasing coupling between the two wells. The fact that the luminescence line of the 40-Å-barrier sample lies above the one of the 60-Å-barrier sample can be explained by a one-monolayer (i.e., 2.83 Å) deviation from the nominal well width. The difference in the ratio of the indirect to the direct transition intensity reflects the difference in barrier width. The smaller the barrier width the higher the tunneling rate from the heavy-hole level in well 2 to that in well 1 and, consequently, the larger the intensity ratio. In fact, in the sample with the narrowest barrier (25 Å) the direct transition is not observed at all.

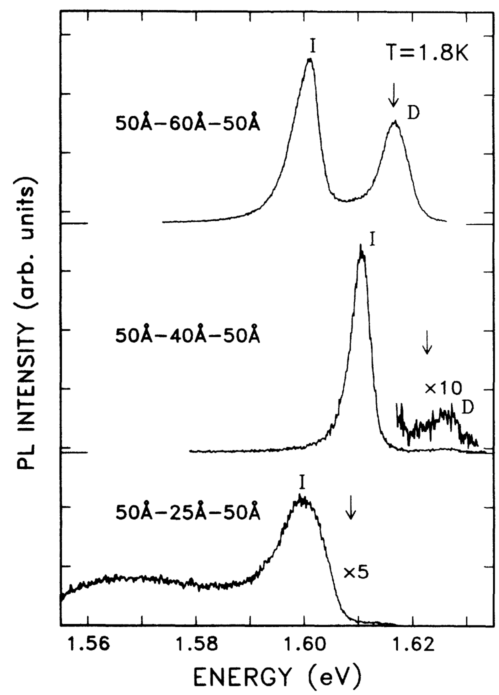

FIG. 2. Time-integrated photoluminescence spectra of 50-Å GaAs DQWs with 25-, 40-, and 60-Å $Al_{0.3}Ga_{0.7}As$ barriers at electric fields of 12.7, 13.9, and 14.2 kV/cm, respectively. The spectra have been shifted vertically for clarity. The arrows indicate the peak positions of the luminescence lines under flat-band conditions. The different energy shifts of the indirect luminescence peaks relative to the direct ones reflect the difference in barrier width. The luminescence band seen at about 1.565 eV in the 50-Å–25-Å–50-Å sample is probably associated to recombination at impurities.

The conversion of externally applied voltage into electric field was done by fitting the energy shift of the indirect transition to the equation $\Delta E = e\mathcal{E}d = ed(V - V_b)/W$, where V is the applied voltage, V_b the built-in voltage, and W the width of the intrinsic region. The values of d, V_b, and W obtained from these fits were in good agreement with the growth parameters.

For the following time-resolved measurements the spectrometer bandpass was set to the peak of the indirect and, when observable, also to the peak of the direct photoluminescence line, unless otherwise mentioned. The bandpass spectral width (full width at half maximum) was 2.5 meV. Figure 3(a) shows decay curves obtained in this way for the indirect exciton luminescence of the 50-Å–40-Å–50-Å sample. As the electric field increases there is a dramatic enhancement of the luminescence decay time.

The zero of the time scale in Fig. 3 was chosen to coincide with the peak of the luminescence decay curve under flat-band conditions which occurs at the end of the laser pulse. However, as the electric field increases, the peak of the indirect luminescence decay curves is delayed [see Fig. 3(a)]. On the other hand, the decay curve of the direct

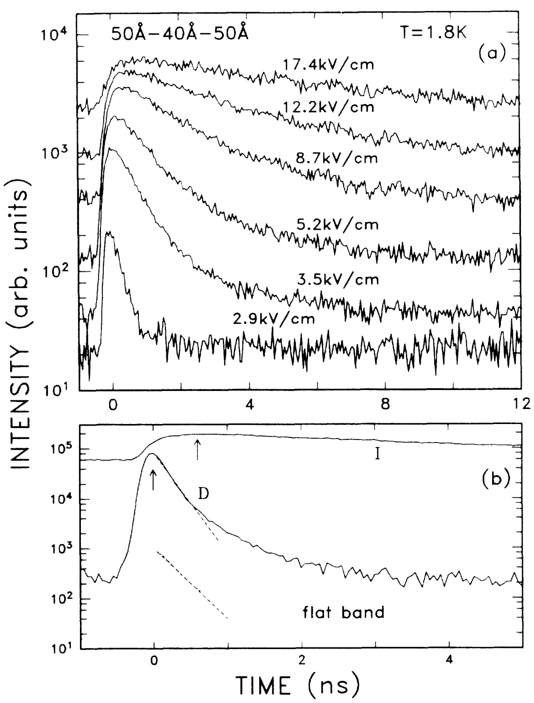

FIG. 3. Time dependence of the photoluminescence for the (50-Å GaAs)/(40-Å $Al_{0.3}Ga_{0.7}As$)/(50-Å GaAs) DQW. (a) Decay curves of the indirect exciton photoluminescence under various electric fields. (b) Time decay of the integrated intensity of the direct (D) and indirect (I) luminescence lines at an electric field of 15.7 kV/cm (solid curves) together with the time decay of the integrated luminescence intensity under flat-band conditions (dashed curve). The spectra have been shifted vertically for clarity. The arrows indicate the peak positions of the direct and indirect luminescence decay curves and the straight lines correspond to exponential fits to the decay curves at short times, from which the exponential decay time was extracted.

luminescence continues to peak at zero, as can be seen in Fig. 3(b). At an electric field of 15.7 kV/cm the indirect luminescence decay curve peaks about 600 ps after the direct luminescence one. We attribute this experimentally significant delay to holes tunneling nonresonantly[21] from well 2 to well 1 [see Fig. 1(b)] and thus further increasing the indirect exciton population after the laser pulse has ended. (The electrons excited into the antisymmetric level relax very fast to the symmetric one.) Furthermore, at 15.7 kV/cm the direct luminescence intensity is decaying faster than the luminescence intensity under flat-band conditions [see Fig. 3(b)] indicating that hole tunneling is contributing to the decay of the direct luminescence.

The delay time of about 600 ps observed for the indirect luminescence decay curve is related to the nonresonant hole tunneling time but is not a good measure of it. It is possible to obtain an estimate of this tunneling time from the decay time of the direct luminescence, τ_d, using the equation $1/\tau_d = 1/\tau_r + 1/\tau_t$, where τ_r is the direct recombination time and τ_t the tunneling time. Assuming that τ_r is not affected by the electric field, we set it equal to 270 ps, which is the value obtained from the slope of the decay curve under flat-band conditions. With $\tau_d = 150$ ps we get $\tau_t = 340$ ps. Fast-decaying curves are influenced by the system response, and the decay times obtained have been corrected for it. Including the errors introduced by this correction results in a possible error as large as a factor of 2 in τ_t.

No similar delay effects of the indirect luminescence decay curves were observed in the 25- and 60-Å-barrier samples, possibly because the tunneling rate is faster than our experimental resolution in the former case and because the tunneling rate is too slow to produce a substantial exciton population increase in the latter. In the 25-Å-barrier sample the direct luminescence line was too weak to be observed. In the 60-Å-barrier sample, as in the 40-Å-barrier sample, the decay time of the indirect luminescence was shorter than the luminescence decay time under flat-band conditions. Using the same arguments as above we obtain $\tau_t = 440$ ps for an electric field of 14.2 kV/cm. Due to the large errors involved a quantitative comparison between the tunneling times for different barriers is not possible.

Nido *et al.*[12] have observed a nonresonant hole tunneling time of the order of 50 ps in a 50-Å–30-Å–100-Å $GaAs/Al_{0.35}Ga_{0.65}As$ asymmetric DQW structure. On the other hand, Leo *et al.*[14] have reported the nonresonant hole tunneling time to be longer than 8 ns in 63-Å–50-Å-90-Å $GaAs/Al_{0.3}Ga_{0.7}As$ DQWs. The nonresonant tunneling time of the order of 300 ps at 15.7 kV/cm determined in this work is in agreement with the theoretical calculations of Bastard *et al.*[18] for impurity-assisted hole tunneling in the same DQW structure (see Fig. 14 in Ref. 18). However, a systematic investigation of resonant and nonresonant hole tunneling rates as a function of barrier thickness is needed.

We now turn to a quantitative presentation of the exciton lifetimes as a function of electric field. The results for the three different barrier thicknesses are summarized in Fig. 4. The experimental points in Fig. 4 were obtained from the slopes of decay curves like the ones shown in Fig. 3(a). In the case of nonexponential decay, probably resulting from fluctuations in the barrier width,[6] the slope at short times was taken. In Fig. 4 we thus plot the fastest decay time. There is considerable error (about $\pm 20\%$) in

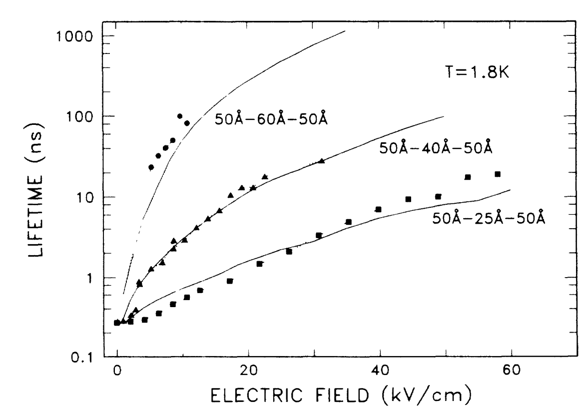

FIG. 4. Lifetime of the spatially indirect excitons as a function of electric field for three different barrier thicknesses: 25, 40, and 60 Å. The solid lines represent theoretical calculations (see text). The dashed lines are drawn as a guide to the eye.

the long lifetimes determined for the 50-Å–60-Å–50-Å sample due to the 13-ns laser-pulse repetition rate. Nevertheless, since these lifetimes are 1 or 2 orders of magnitude longer than the ones measured for a 40-Å barrier at the same electric field, a comparison is still valid.

The integrated luminescence intensity is approximately the same for all three samples and is almost constant as a function of electric field. We therefore assume that the influence of nonradiative processes even on the longest measured exciton lifetimes is small. In the 25-Å-barrier sample the decay time at the peak of the impurity-related luminescence band was also measured and was found to exceed the decay time at the peak of the intrinsic luminescence for low electric fields. The impurity-related decay time increased at a faster pace with electric field and became an order of magnitude longer at high fields. Thus, the measured lifetimes are dominated by the intrinsic recombination time.

As can be seen from Fig. 4, in the 50-Å–40-Å–50-Å sample an electric field of 30 kV/cm causes the measured recombination lifetime to increase by about 2 orders of magnitude. For a 25-Å barrier, more than twice this electric field is necessary to produce the same effect, whereas for a 60-Å barrier already half this electric field causes an increase of almost 3 orders of magnitude. The experimental results are compared with theoretical calculations presented as solid lines in Fig. 4. The electron and heavy-hole wave functions were calculated as a function of electric field by numerically solving Schrödinger's equation and the radiative recombination lifetime τ was evaluated according to the equation $\tau \propto 1/[|M_{e\text{-}h}|^2 |f(0)|^2]$, where $M_{e\text{-}h}$ is the overlap integral of the electron and hole wave functions and $f(r)$ the exciton envelope function (for details see Ref. 7).[22] The wider the barrier the smaller the overlap integral at a certain electric field and thus the longer the recombination lifetime, leading to lifetimes as long as 1.1 μs for an electric field of 35 kV/cm in the 60-Å-barrier sample. All three theoretical curves were calculated with only one adjustable parameter, the proportionality coefficient in the above equation. The good agreement between theory and experiment further supports our assumption that the measured lifetimes are dominated by the radiative recombination times.

In conclusion, we have conducted a systematic study of the recombination lifetime of spatially indirect excitons in $GaAs/Al_{0.3}Ga_{0.7}As$ double quantum wells as a function of electric field and barrier thickness. A theoretical model that calculates the electron and hole wave-function overlap including excitonic effects predicts lifetimes which are in good quantitative agreement with the experimental results. On the other hand, the lifetime of the spatially direct excitons is shorter than the lifetime under flat-band conditions due to holes tunneling from one well to the other. In the case of a 40-Å barrier, the nonresonant hole tunneling time was found to be of the order of 300 ps, in agreement with recent theoretical calculations.[18]

The lifetimes of spatially indirect excitons measured here are enhanced by 2 to 3 orders of magnitude relative to the lifetimes under flat-band conditions. The electric field necessary to produce a given lifetime enhancement depends, however, on the barrier thickness. Therefore, in order to elucidate the mechanisms by which the electric field induces the linewidth reduction observed in Ref. 8, a detailed investigation of this reduction in structures with different barrier thicknesses is necessary.

We thank S. S. Kano for valuable discussions on the exciton envelope function, L. Esaki for a critical reading of the manuscript, and M. S. Christie for sample preparation.

---

[1]H.-J. Polland *et al.*, Phys. Rev. Lett. **55**, 2610 (1985).

[2]Y. J. Chen *et al.*, Phys. Rev. B **36**, 4562 (1987), and references therein.

[3]J. E. Golub *et al.*, Appl. Phys. Lett. **53**, 2584 (1988), and references therein.

[4]S. Charbonneau *et al.*, Phys. Rev. B **38**, 6287 (1988).

[5]T. B. Norris *et al.*, Phys. Rev. B **40**, 1392 (1989).

[6]J. E. Golub *et al.*, Phys. Rev. B **41**, 8564 (1990).

[7]T. Fukuzawa *et al.*, Surf. Sci. **228**, 482 (1990); T. Fukuzawa, T. K. Gustafson, and E. Yamada, IEEE J. Quantum Electron. **QE-26**, 811 (1990).

[8]T. Fukuzawa, E. E. Mendez, and J. M. Hong, Phys. Rev. Lett. **64**, 3066 (1990).

[9]E. E. Mendez *et al.*, Appl. Phys. Lett. **47**, 415 (1985).

[10]H. W. Liu *et al.*, Appl. Phys. Lett. **54**, 2082 (1989).

[11]H. Schneider *et al.*, Phys. Rev. B **40**, 10040 (1989).

[12]M. Nido *et al.*, Appl. Phys. Lett. **56**, 355 (1990).

[13]N. Vodjdani *et al.*, Appl. Phys. Lett. **56**, 33 (1990).

[14]K. Leo *et al.*, in *Proceedings of the International Society for Optical Engineering,* SPIE Conference Proceedings No. 1283 (SPIE, Bellingham, WA, to be published); K. Leo *et al.*, Phys. Rev. B **42**, 7065 (1990).

[15]J. B. Xia, Phys. Rev. B **38**, 8365 (1988).

[16]R. Wessel and M. Altarelli, Phys. Rev. B **39**, 12802 (1989).

[17]E. T. Yu, M. K. Jackson, and T. C. McGill, Appl. Phys. Lett. **55**, 744 (1989).

[18]G. Bastard *et al.*, J. Lumin. **44**, 247 (1989).

[19]See, for example, F. Capasso, K. Mohammed, and A. Y. Cho, IEEE J. Quantum Electron. **QE-22**, 1853 (1986).

[20]W. G. McMullan, S. Charbonneau, and M. L. W. Thewalt, Rev. Sci. Instrum. **58**, 1626 (1987).

[21]We are speaking about nonresonant hole tunneling since resonance with the light-hole level would occur at 33 kV/cm according to the heavy-hole–light-hole splitting of 30 meV determined from photoluminescence excitation spectroscopy.

[22]The material parameters used in the calculations are the following: valence-band discontinuity $\Delta E_v = 130.9$ meV, conduction-band discontinuity $\Delta E_c = 243.2$ meV, electron effective mass for GaAs and $Al_{0.3}Ga_{0.7}As$ $m_e = 0.0665 m_0$ and $0.0915 m_0$, respectively, and heavy-hole effective mass for GaAs and $Al_{0.3}Ga_{0.7}As$ $m_{hh} = 0.377 m_0$ and $0.4074 m_0$, respectively, where m_0 is the free-electron mass.